Inorganic Chemistry Communications 142 (2022) 109696

Contents lists available at ScienceDirect

Inorganic Chemistry Communications

journal homepage: www.elsevier.com/locate/inoche

Short communication

Synthesis of benzotriazole functionalized ZIF-8 by postsynthetic modification for enhanced CH_4 and CO_2 uptakes

Mustafa Erkartal [a,*], Kaan Incekara [b], Unal Sen [b]

[a] Department of Nanotechnology, Abdullah Gul University, Kayseri 38080, Turkey
[b] Departmentof Materials Science and Engineering, Eskisehir Technical University, Eskisehir 26555, Turkey

ARTICLE INFO

Keywords:
Nanoparticles
Porous materials
Surfaces
Metal-organic frameworks
Post-synthetic modification

ABSTRACT

In this work, a series of functionalized ZIF-8 were synthesized via incorporation of benzotriazole ligands into the framework with a post-synthetic method. The crystal structure and porosity were preserved for all functionalized samples. Although a relatively low percentage of ligand exchange (approximately 10–22%) was observed due to steric and kinetic effects, a remarkable improvement was found in CO_2 and CH_4 uptake capacities due to the incorporation of more polar N sites into the structure and the change in pore size of the frameworks. The resulting ZIF-8-S5 exhibited 45.17(CO_2) and 15.08 (CH_4) $cm^3\ g^{-1}$ at 273 K under 1.2 bar, which corresponds to an enhancement of 20 and 35% compared to pristine ZIF-8. Further, all functionalized samples showed the significant improvement of selective CO_2 over N_2.

1. Introduction

Zeolitic imidazolate frameworks (ZIFs), a sub-class of metal–organic frameworks (MOFs), are isomorphous with zeolites, and they usually exhibit exceptional chemical and thermal stabilities [1]. MOFs (also ZIFs) have the tailorable structure—that is, their properties can be finely tuned by using a substituted organic ligand and secondary building units. Among the various strategies, the solvent-assisted linker exchange (SALE) is a facile and versatile process for functionalization of MOFs to improve their catalytic performance, gas sorption and electrochemical properties [2]. To date, this strategy has been utilized in the synthesis or functionalization of many ZIFs [3–7]. However, the main challenge for ligand exchange is introducing new ligands with more coordinative atoms into the framework [3].

Benzotriazole (BtaH) and its conjugate base, benzotriazolate anion (Bta), is a versatile ligand existing three adjacent donor sites. It is a weak acid (pKa = 8.38) and exists as a mixture of tautomeric forms (Fig. 1**a-b**) [8]. To date, several BtaH-transition metal coordination compounds have been reported, in which it has been observed that BtaH showed monodentate, bidentate and tridentate coordination modes [9]. However, all these structures were dense and did not show the accessible porosity.

It has shown that the introducing of uncoordinated nitrogen-donor groups in to frameworks could improve selective CO_2 adsorption and CH_4 storage of MOFs [10–14]. Also, methyl-functionalized MOFs have been shown to display enhanced CO_2 uptake affinity [15]. Inspired these observations, herein, it was aimed to incorporate BtaH and 5-methyl-1H-benzotriazole (5-Me-BtaH) ligands to the ZIF-8 structure with SALE method. Thus, it was hypothesized that CO_2 capture and CH_4 storage capacity and also gas selectivity would improve under ambient conditions due to the integration of BtaH or 5-Me-BtaH into the structure with bidentate coordination, and, as a result, active N or N and methyl sites on the pore surface of ZIF-8 (Fig. 1**c**).

2. Experimental

The as-synthesized ZIF-8 (0.437 mmol) was dispersed in 5 mL DMF and BtaH (0.874 mmol) was dissolved in 10 mL DMF. Then second solution was poured into first. The resultant mixture was transferred to a 28 mL screw cap vial. The vial placed in an isothermal oven at 80 °C for 48 h. After cooling down to room temperature, the SALE product was isolated centrifugation (9000 rpm, 20 min) and washed with DMF (2 × 15 mL) and methanol (2 × 15 mL). The obtained powder firstly dried under ambient conditions and then activated at 120 °C in a vacuum oven. The same procedure was used for 5-Me-BtaH (**SI**).

* Corresponding author.
E-mail address: merkartal@mail.com (M. Erkartal).

https://doi.org/10.1016/j.inoche.2022.109696
Received 10 May 2022; Received in revised form 10 June 2022; Accepted 18 June 2022
Available online 21 June 2022

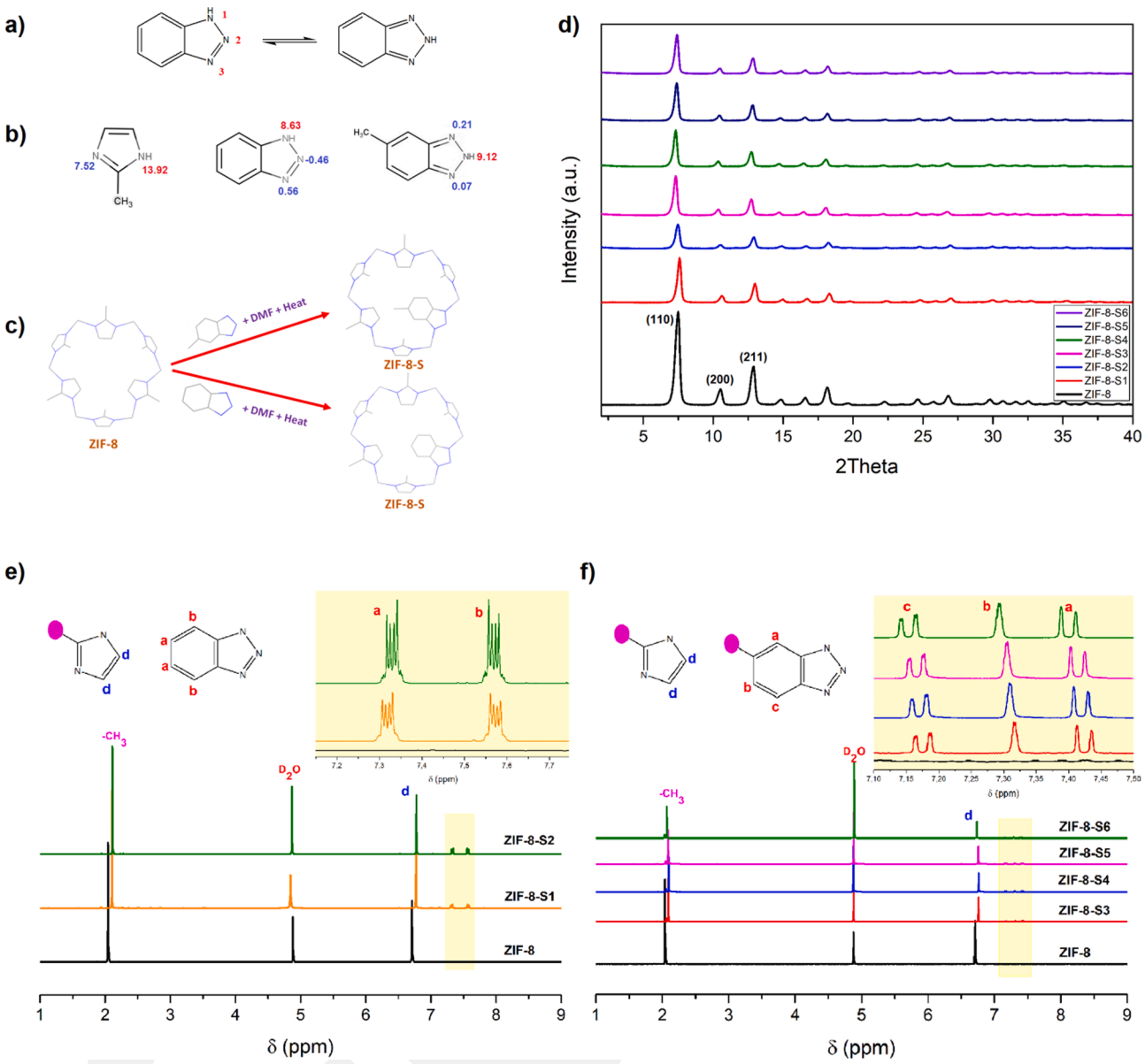

Fig. 1. (a) Tautomerism in BtaH, (b) pKa values of the ligands, (c) a schematic for the SALE mechanism, (d) XRD patterns of the samples, (e-f) ^{1}H NMR of the samples.

3. Results and Discussion

The XRD patterns of functionalized samples well match with the pristine ZIF-8, indicating that crystal structure of the framework was maintained during the SALE process in DMF (Fig. 1**d**). However, an amorphization was observed for the further increase in daughter ligand (BtaH or 5-Me-BtaH) concentrations (**Fig. S2**). Surprisingly, the partial amorphization was observed in ZIF-67 (a cobalt analogue of ZIF-8) under same experiments conditions even at lower low daughter ligand concentrations, while a complete amorphization was encountered at higher concentrations (**Fig. S3**). Therefore, the scope of this study was limited to ZIF-8 only.

The progress of SALE was monitored by digestive 1H NMR (Fig. 1**e-f**, also **Fig S5-S11**). The singlets at around 2.11 and 6.78 ppm observed in all samples represent – CH_3 and CH=CH of 2-methylimiazole (mIm) protons, respectively. The peaks observed between 6.6 and 7.4 ppm with the incorporation of the daughter ligand to the frameworks correspond to the benzylic protons of the benzotriazole-based ligands. Calculations revealed that integration of daughter ligand into ZIF-8 is between 11 and 22 % and slightly increases with an increase of daughter ligand concentration in reaction medium **(SI).** In the view of chemical kinetic, a lower pKa for the daughter ligand is typically required since pKa difference in the "N–H" bonds broken and formed can be a measure for the equilibrium constant of the exchange reaction. For this study, both BtaH (pKa = 8.63) and 5-Me-BtaH (pKa = 9.12) have lower pKa values than mIm (pKa = 13.92) which promotes the SALE reaction [3,10]. On the other hands, steric constraints can be the reason for such lower ligand exchange ratios [16]. FTIR also utilized to verify the secondary ligand in ZIF-8 (**Fig. S12**). The new peaks observed at around 1270 and 790 cm^{-1} in the functionalized frameworks correspond to CH in-plane and out-of-plane bending due to the fused benzene ring [8]. Thermogravimetric analysis (TGA) measurements showed that although benzotriazole functionalized samples are stable up to 300–400 °C depending on daughter ligand content they are less thermally stable than pure ZIF-8 under air (**Fig S13**).

Fig. 2**a** shows the nitrogen adsorption/desorption isotherms of all samples at 77 K. All frameworks exhibit a typical type-I isotherm which is characteristic for adsorbents that contain micropores only (Fig. 2**b**). It

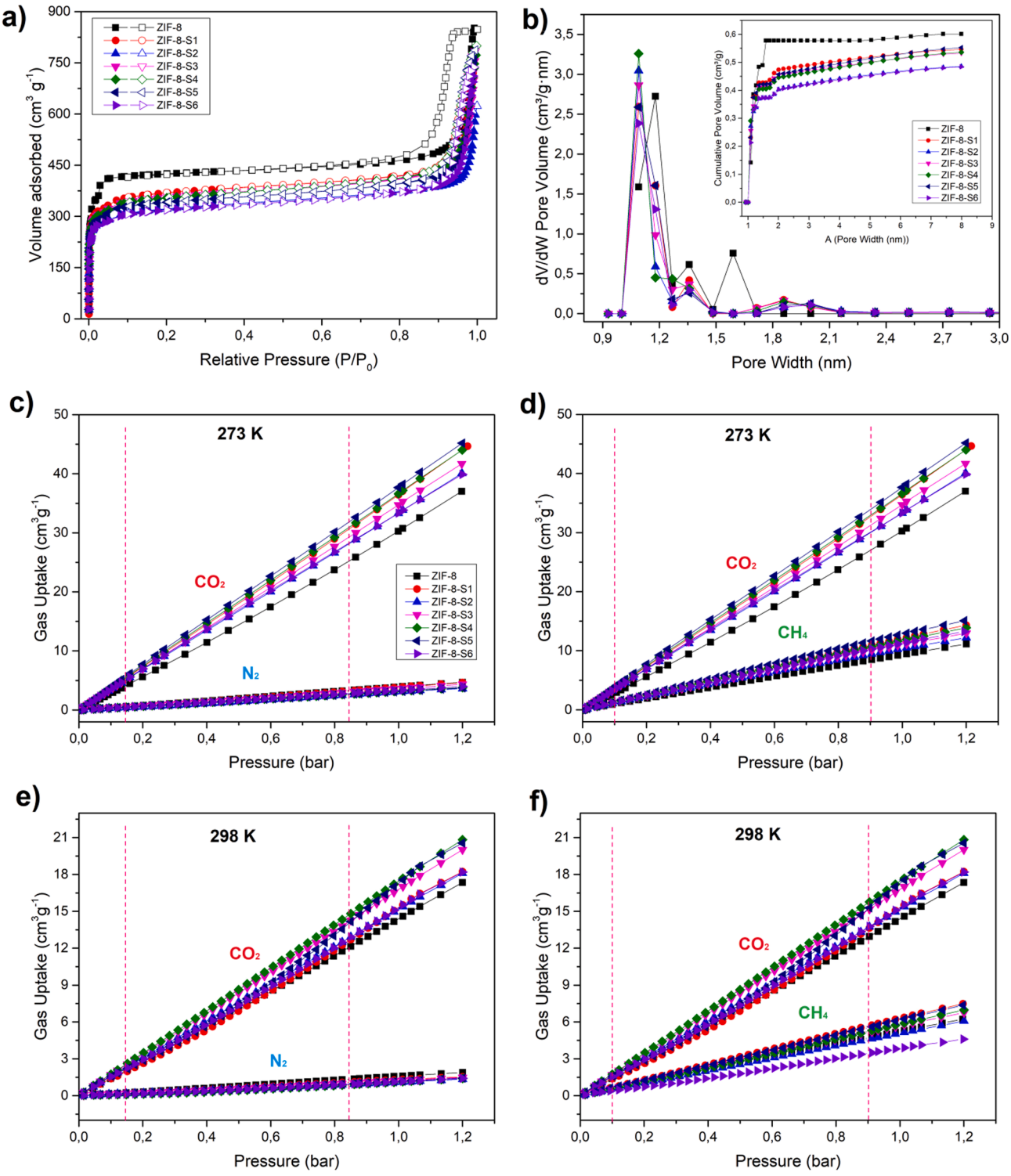

Fig. 2. (a) N_2 isotherms at 77 K, (b) DFT pore sizes and volumes, (c-d) low pressure CO_2,CH_4 and N_2 isotherms at 273 K, (e-f) low pressure CO_2,CH_4 and N_2 isotherms at 298 K. (The dashed lines show the partial pressures of the gases used for selectivity calculations.).

is evident that the amount of adsorbed nitrogen and thus the specific surface area (SSA) and pore volumes of the frameworks decrease with the incorporation of the secondary ligand into the structure. For example, the SSA of pristine ZIF-8 is 1744 $m^2\ g^{-1}$, while ZIF-8-S2 and ZIF-8-S6 are 1221 and 1210 $m^2\ g^{-1}$ respectively. The steric effects arising from incorporation of a bulky BtaH ligand into the structure may be responsible for this decrease in SSA [17].

Although post-synthetic modifications, such as the SALE, cause a decrease in the surface area of MOFs, active nitrogen and open metal sites due to structural defects that may occur as a result of SALE can increase the CO_2 and CH_4 adsorption capacities [10,18]. Hence, low-pressure CO_2 and CH_4 isotherms of all materials in this study at 273 and 298 K were conducted twice, taking into account reproducibility (Fig. 2**c-f**). For ZIF-8, the CO_2 uptakes were measured as 37.02 and 17.35 cm^3g^{-1} at 273 and 298 K under 1.2 bar, respectively. As expected, the CO_2 uptake capacity of all functionalized materials improved.

Table 1
Gas uptakes values of the samples. (For the ZIF-8-S1 and S2 daughter ligand is BtaH and it is 5-Me-BtaH for others).

MOF	Linker Exchange (%)	BET S.A. ($cm^3\ g^{-1}$)	Pore.Volume ($cm^3 g^{-1}$)	CO_2 (273 K /298 K)	CH_4 (273 K /298 K)	SCO_2/N_2 (273/298 K)	SCO_2/CH_4 (273/298 K)
ZIF-8	–	1744	0.60	37.02/17.35	11.14/6.23	7.11/8.80	3.17/2.62
ZIF-8-S1	13	1407	0.54	44.66/18.23	14.33/7.47	9.81/10.19	3.16/2.19
ZIF-8-S2	22	1221	0.48	40.07/18.10	12.19/6.07	11.14/14.35	3.32/3.08
ZIF-8-S3	11	1361	0.53	41.67/20.01	12.97/6.75	9.83/14.21	3.27/2.99
ZIF-8-S4	14	1350	0.53	44.01/20.83	13.88/6.97	11.79/14.89	3.24/3.00
ZIF-8-S5	15	1306	0.53	45.17/20.56	15.08/7.36	12.31/13.20	3.00/2.71
ZIF-8-S6	17	1210	0.48	39.88/18.19	13.25/4.60	10.47/13.70	3.08/4.01

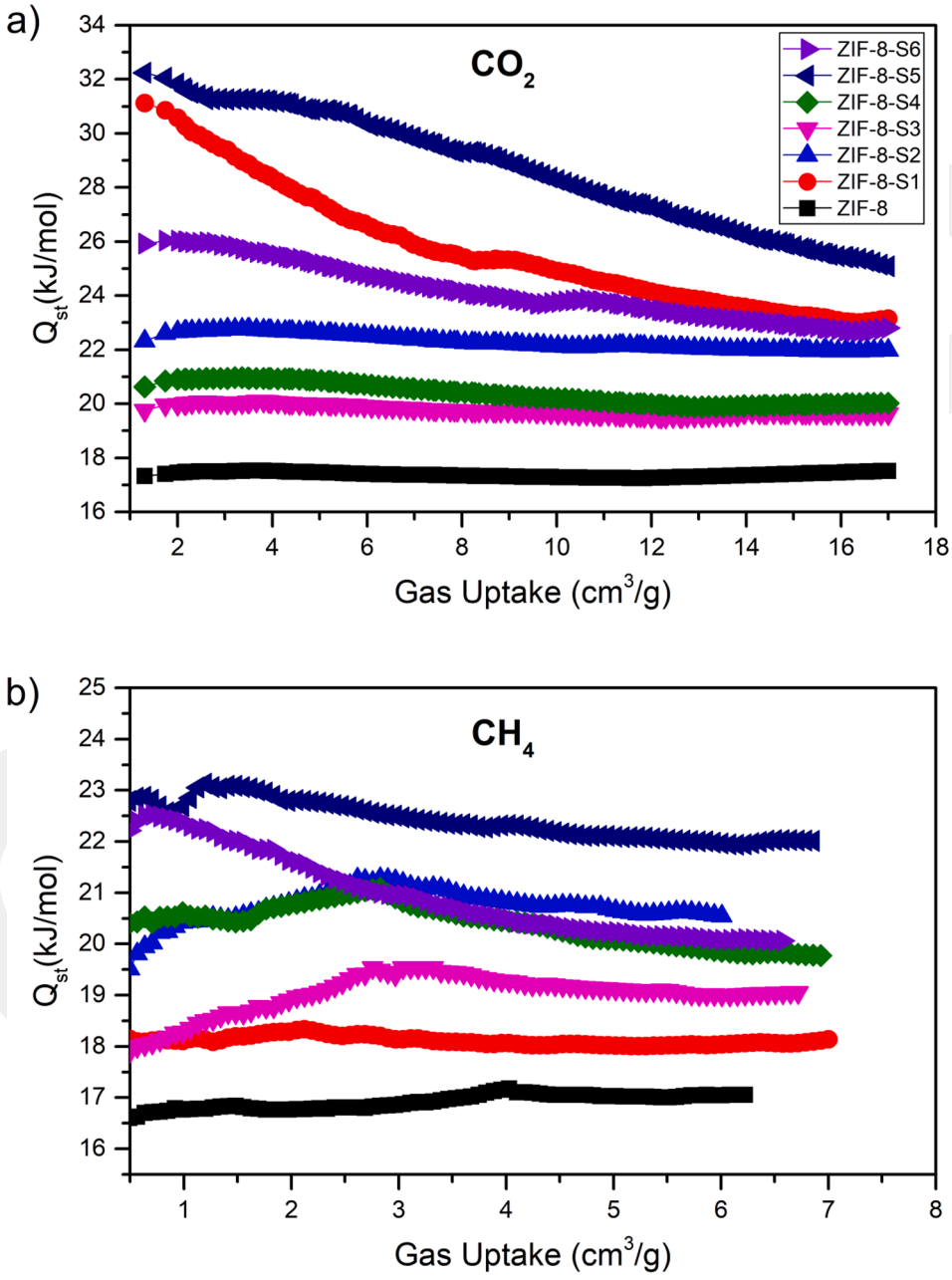

Fig. 3. Isosteric heats of adsorptions (Q_{st}) as a function of gas loading in $cm^3\ g^{-1}$ for (a) CO_2 and (b) CH_4.

Among them, the ZIF-8-S5 is capable of adsorbing 45.17 and 20.56 $cm^3 g^{-1}$ of CO_2 at 273 and 298 K under 1.2 bar, which corresponds to an improvement of more than 20%. Similar enhancement trend was observed for CH_4 uptakes of the samples. ZIF-8-S5 attained a high CH_4 uptake of 15.08 and 7.36 $cm^3 g^{-1}$ at 273 and 298 K under 1.2 bar. Compared to ZIF-8, this corresponds to an enhancement of 35%. The selective CO_2 adsorption upon N_2 and CH_4 for all of the samples also were calculated from the pure gas isotherms by considering partial

pressures of gas mixtures [19]. ZIF-8-S5 showed the highest CO_2/N_2 selectivity which is almost two times higher than that of pure-phase ZIF-8 (Table 1).

To further understand the adsorption properties, the isosteric heats of adsorption, Q_{st}, were determined from the CO_2 and CH_4 adsorption isotherms at 273 and 298 K under ambient pressure. Q_{st} of CO_2 for pristine ZIF-8 was determined as ≈ 17 kj mol^{-1} regardless of the amount of CO_2 absorbed. This indicates that ZIF-8 has uniform adsorption sites and shows a relatively weak binding energy and low CO_2 uptake because of its coordinatively saturated metal sites. As can be observed from Fig. 3**a**, Q_{st} values of functionalized samples are much higher than that of ZIF-8. This implies that integration of functionalized linkers into the framework improve the adsorption affinity for CO_2. Also, the trend in the Q_{st} values is clearly in compliance with the uptake amounts of the order of the samples. However, the shape of Q_{st} curves of the functionalized samples, especially for ZIF-8-S1 and ZIF-8-S5, are quite different that of ZIF-8. As the more energetic sites are preferentially populated first by the adsorbate, both ZIF-8-S1 and ZIF-8-S5 have a high Q_{st} at low coverage. A continuous decrease in Q_{st} is observed as the adsorbate molecules occupy adsorption sites but this reduction deviates from linearity in the studied region for both materials. This would appear to indicate that functionalized samples have the non-uniform pore size distribution and heterogonous adsorption sites in terms of their energy. The Q_{st} of CH_4 for all seven materials evaluated in this work plotted in Fig. 3**b**. The framework with the highest volumetric CH_4 adsorption, namely ZIF-8-S5- has the highest adsorption enthalpy. The low-coverage Q_{st} of ZIF-8-S5 (23 kj mol^{-1} is nearly fifty percent higher than the value of Q_{st} of pure ZIF-8 (16 kj mol^{-1}), confirming strong interactions between methane and the framework [20]. For ZIF-8-S5, Q_{st} of CH_4 first slowly decreases and then increases rapidly with methane loadings. This support the idea that the methane-methane interaction in addition to the methane-framework interaction becomes dominant at high loadings as reported for other MOFs [21,22]. Overall, the suitable pore spaces, high density of accessible N sites, and open zinc sites within ZIF-8-S5 may be the main reason for high methane storage.

4. Conclusion

In summary, a series of functionalized ZIF-8-S were synthesized by the SALE method. Incorporation of BtaH and 5-Me-BtaH into the framework significantly improved the CO_2 and CH_4 uptakes. The main reason behind this can be the incorporation of the secondary ligand into the framework in bidentate mode, resulting in the formation of active N sites on the pore surfaces. Additionally, a decrease in pore volume/window due to the integration of a bulky ligand can be resulted in an enhancement in selective gas uptake.

CRediT authorship contribution statement

Mustafa Erkartal: Conceptualization, Investigation, Writing – review & editing, Supervision, Validation, Project administration. **Kaan Incekara:** Investigation, Validation. **Unal Sen:** Supervision, Validation, Project administration.

Declaration of Competing Interest

The authors declare that they have no known competing financial interests or personal relationships that could have appeared to influence the work reported in this paper.

Acknowledgments

This study was supported by the TUBITAK-1001 project (120 M698).

Appendix A. Supplementary material

Supplementary data to this article can be found online at https://doi.org/10.1016/j.inoche.2022.109696.

References

[1] K.S. Park, Z. Ni, A.P. Cote, J.Y. Choi, R.D. Huang, F.J. Uribe-Romo, H.K. Chae, M. O'Keeffe, O.M. Yaghi P Natl Acad Sci USA 103(27) (2006) 10186-10191.
[2] O. Karagiaridi, W. Bury, J.E. Mondloch, J.T. Hupp, O.K. Farha, Angew Chem. Int. Edit. 53 (18) (2014) 4530–4540.
[3] O. Karagiaridi, M.B. Lalonde, W. Bury, A.A. Sarjeant, O.K. Farha, J.T. Hupp, J. Am. Chem. Soc. 134 (45) (2012) 18790–18796.
[4] C.I. Yen, S.M. Liu, W.S. Lo, J.W. Wu, Y.H. Liu, R.J. Chein, R.Q. Yang, K.C.W. Wu, J. R. Hwu, N.H. Ma, F.K. Shieh, Chem. Eur. J. 22 (9) (2016) 2925–2929.
[5] J.Q. Jiang, C.X. Yang, X.P. Yan, Chem. Commun. 51 (30) (2015) 6540–6543.
[6] C.X. Miao, C.L. Zhou, H.E. Wang, K. Zhu, K. Ye, Q. Wang, J. Yan, D.X. Cao, N. Li, G. L. Wang, J. Power Sources 490 (2021).
[7] J.P. Song, L. Wu, W.D. Dong, C.F. Li, L.H. Chen, X. Dai, C. Li, H. Chen, W. Zou, W. B. Yu, Z.Y. Hu, J. Liu, H.E. Wang, Y. Li, B.L. Su, Nanoscale 11 (14) (2019) 6970–6981.
[8] S.G. Aziz, S.A. Elroby, A. Alyoubi, O.I. Osman, R. Hilal, J. Mol. Model 20 (2014) 3.
[9] C.Z. Ruan, R. Wen, M.X. Liang, X.J. Kong, Y.P. Ren, L.S. Long, R.B. Huang, L. S. Zheng, Inorg. Chem. 51 (14) (2012) 7587–7591.
[10] M. Erkartal, U. Erkilic, B. Tam, H. Usta, O. Yazaydin, J.T. Hupp, O.K. Farha, U. Sen. Chem. Commun. 53 (12) (2017) 2028–2031.
[11] M.X. Zhang, H.H. Cui, L.F. Zhang, G.P. Qin, P.P. Zhang, S. Wang, G.M. Jiang, J. Wang, M.M. Wang, M. Wang, T.M. Sun, Y.F. Tang, Inorg. Chem. 60 (20) (2021) 15646–15652.
[12] Y.X. Ye, H. Zhang, L.J. Chen, S.M. Chen, Q.J. Lin, F.F. Wei, Z.J. Zhang, S.C. Xiang, Inorg. Chem. 58 (12) (2019) 7754–7759.
[13] Z.Z. Jiang, Y. Zou, T.T. Xu, L.H. Fan, P. Zhou, Y.B. He Dalton T 49(11) (2020) 3553–3561.
[14] T.T. Xu, L.H. Fan, Z.Z. Jiang, P. Zhou, Z.R. Li, H.Y. Lu, Y.B. He Dalton T 49(21) (2020) 7174-7181.
[15] H. Liu, Y.G. Zhao, Z.J. Zhang, N. Nijem, Y.J. Chabal, H.P. Zeng, J. Li, Adv. Funct. Mater. 21 (24) (2011) 4754–4762.
[16] M.B. Lalonde, J.E. Mondloch, P. Deria, A.A. Sarjeant, S.S. Al-Juaid, O.I. Osman, O. K. Farha, J.T. Hupp, Inorg. Chem. 54 (15) (2015) 7142–7144.
[17] X.L. Ma, D.F. Liu, Crystals 9 (1) (2019).
[18] Y.W. Abraha, C.W. Tsai, J.W.H. Niemantsverdriet, E.H.G. Langner Acs Omega 6 (40) (2021) 26821–26821.
[19] M. Erkartal, U. Sen Acs Appl. Mater. Inter 10 (1) (2018) 787–795.
[20] J.A. Mason, M. Veenstra, J.R. Long, Chem. Sci. 5 (1) (2014) 32–51.
[21] G. Barin, V. Krungleviciute, D.A. Gomez-Gualdron, A.A. Sarjeant, R.Q. Snurr, J. T. Hupp, T. Yildirim, O.K. Farha, Chem. Mater. 26 (5) (2014) 1912–1917.
[22] W. Zhou, H. Wu, M.R. Hartman, T. Yildirim, J. Phys. Chem. C 111 (44) (2007) 16131–16137.